PREPARATION AND SOME PROPERTIES OF N-TYPE $Ir_xCo_{1-x}Sb_3$ S01,11) SOLUTIONS

Thierry Caillat, C.E. Allevato, Jean-Pierre Fleurial and Alex Borshchevsky
Jet Propulsion Laboratory
California Institute of Technology
Pasadena, CA 91109
(818) 354-0407

Abstract

A number of studies have been recently devoted to the preparation and characterization of binary skutterudite materials to investigate their potential as advanced thermoelectric materials. These studies show that the potential of these binary skutterudite compounds is limited because of their relatively large thermal conductivity. In order to achieve high thermoelectric figure of merits for these materials, efforts should focus on thermal conductivity reduction. Recent results obtained on n-type $CoSb_3$ and $IrSb_3$ compounds have shown that n-type skutterudite materials might have a better potential for thermoelectric applications than p-type materials. The thermoelectric properties of p-type $Ir_xCo_{1-x}Sb_3$ solid solutions have been recently investigated and it was shown that a substantial reduction in thermal conductivity was achieved. We prepared and measured some properties of n-type $Ir_xCo_{1-x}Sb_3$ solid solutions. The samples are characterized by large Seebeck coefficient values and significantly lower thermal conductivity y values than those measured on the binary compounds $CoSb_3$ and $IrSb_3$. A maximum ZT value of about 0.4 was obtained at a temperature of about 300°C. Improvements in the figure of merit are possible in this system by optimization of the doping level.

INTRODUCTION

Skutterudite materials have generated a considerable interest as new thermoelectric materials over the past few years. The work was first initiated at the Jet Propulsion Laboratory (JPL) and initially concentrated on the binary compounds $IrSb_3$ and $CoSb_3$ (Caillat et al., 1992). Since then, a number of studies have been reported on the preparation and transport properties of binary skutterudite compounds AB_3 with A=Ir, Rh or Co and B=As, Sb or P. These studies showed that these compounds are semiconductors with interesting transport properties, especially high hole mobilities. However, the thermoelectric figure of merit of the binary compounds is limited by their relatively high thermal conductivity. A typical room temperature value for $IrSb_3$ and $CoSb_3$ is about 110 $mW.cm^{-1}.K^{-1}$ (Caillat et al., 1995a and 1995b) (Morelli et al., 1995). Several approaches have already been considered to reduce the lattice thermal conductivity in this class of materials. The first approach, used for many state-of-the-art thermoelectric materials, is to form solid solutions between isostructural compounds and reduce the lattice thermal conductivity by increasing the point defect scattering. The preparation and characterization of p-type $Ir_xCo_{1-x}Sb_3$ solid solutions have been studied (Borshchevsky et al., 1995) and the results have shown that a reduction of about 70% is achieved for a solid solution with about 12 mole% of $CoSb_3$. Another approach which has been considered to lower the lattice thermal conductivity of skutterudite materials is to study the so-called "filled" skutterudites. in these materials, a rare element R is inserted in the voids of the unfilled structure resulting in the formula RM_4B_{12} where M=Fe, Ru or 0s and B= P, As or Sb. This element would substantially scatter the phonons, resulting in low thermal conductivity values. Recent studies have shown that low lattice thermal conductivity values can be obtained for such materials (Nolas et al., 1995) (Tritt et al., 1995) (Morelli and Meisner 1995). However, more work is needed on these materials to improve their electrical properties and fully assess their potential for thermoelectric applications.

Although significant reduction in lattice thermal conductivity were obtained for p-type $Ir_xCo_{1-x}Sb_3$ solid solutions, the thermoelectric figure of merit of these solid solutions is limited mainly because of their relatively low Seebeck coefficient values. We determined that n-type $CoSb_3$ might have a better potential for high ZT values because the electron effective mass is at least one order of magnitude larger than the hole effective mass in this material, resulting in large n-type Seebeck coefficient values (Caillat et al., 1995b). However, the thermoelectric figure of merit of n-type $IrSb_3$ and $CoSb_3$ is limited by their relatively large thermal conductivity. N-type $Ir_xCo_{1-x}Sb_3$ solid solutions should have better thermoelectric properties based on lattice thermal conductivity reduction obtained for p-type $Ir_xCo_{1-x}Sb_3$ solid solutions. We report in this paper on the preparation of n-type $Ir_xCo_{1-x}Sb_3$ solid solution

samples and preliminary measurements of their thermoelectric properties are also presented.

EXPERIMENTAL

No quasibinary alloying behavior was expected due to the incongruent melting character of the compounds (peritectic decomposition temperature of 1141°C for $IrSb_3$ and 929°C for $CoSb_3$). Also the difference in lattice parameter between the two compounds is substantial, about 2.3'%.. However, it was shown that a partial solid solution exist between $IrSb_3$ and $CoSb_3$ and there is a miscibility gap in the system $Co_xIr_{1-x}Sb_3$ for $0.2<x<0.65$. Samples were prepared by a liquid-solid phase sintering (LSPS) technique from elemental powders in amounts close to stoichiometric ratios. Flat bottom 6.35 mm ID quartz ampoules were carbon coated on the inside by cracking acetone and then annealed for a short period of time in vacuum. Elemental powders of Ir, Co and dopants were mixed and placed at the bottom of the ampoules. 'Then, Sb shots were added on top, the ampoules were scaled under vacuum (10-5 I'err), The ampoules were then heated up to 800°C for Co-rich solid solutions and up to 950°C for Ir-rich solid solutions and held at these temperatures for 24 hours. During the process, melted Sb diffused through the metal powders and samples about 6.3 mm in diameter and up to 15 mm long were obtained. The density of the samples was found to be bet ween 85 and 92% of their respective theoretical density. The properties of three different compositions were investigated: one Jr-rich solid solution ($Co_{0.12}Ir_{0.88}Sb_3$) with Pt as dopant and two Co-rich solid solutions, $Co_{0.94}Ir_{0.06}Sb_3$ and $Co_{0.88}Ir_{0.12}Sb_3$ with Tc or Pt as dopant.

Samples, polished by standard metallographic techniques, were investigated using an optical microscope with and without light polarization or Nomarski contrast to observe their quality and homogeneity. Microprobe analysis (MPA) was performed on selected samples to determine their atomic composition and the dopant concentration using a JEOL JXA-733 electron superprobe operating at 20 kV of accelerating potential and 25x10-9 A of probe current. Pure elements (purity better than 99.80A) were used as standards and X-my intensity measurements of peak and background were conducted by wavelength dispersive spectrometry. Mass densities were determined using the immersion technique. Because of the substantial porosity found, I .SPS samples were held for at least 30 minutes in toluene before weighing to allow the liquid to penetrate the pores. A Siemens D-500 diffractometer produced diffractometry patterns at room temperature. Small additions of Si powders were made to some samples as an internal standard.

The electrical and thermal transport properties of the samples investigated were measured in the 25-500°C temperature range. The electrical resistivity and the Hall coefficient were measured by the Van der Pauw method using tungsten probes located on the top surface of the sample as close as possible to the sample's edge (typically a 1 mm thick, 6.35 mm diameter slice). The Seebeck coefficient measurements were conducted by creating a variable temperature difference across the sample and measuring the corresponding linear variation of its thermoelectric voltage. Large samples are usually measured by this technique but samples as thin as 1 mm can also be accommodated. The thermal diffusivity and the heat capacity of selected samples were measured by a flash diffusivity technique. The thermal conductivity was calculated from the measured density, thermal diffusivity and heat capacity values.

RESULTS AND DISCUSSION

MPA and X-ray results showed that $Co_xIr_{1-x}Sb_3$ samples with x=0. 12, 0.04 and 0.88 were single phase, in agreement with our previous results on p-type $Co_xIr_{1-x}Sb_3$ solid solutions (Borshchevsky et al., 1995). Some room temperature properties of several n-type $Co_xIr_{1-x}Sb_3$ samples are listed in Table 1. The room temperature Hall mobilities of some solid solution samples are compared to the values for n-type $IrSb_3$ and $CoSb_3$ in Figure 1.

TABLE 1. Some Room Temperature Properties of n-type $Co_xIr_{1-x}Sb_3$ Samples: p = electrical resistivity (mΩ.cm), n = carrier concentration (cm^{-3}), μ = electron mobility ($cm^2/V.s$) and α = Seebeck coefficient (pV/K).

Sample	Nominal composition	p	n	μ	α
2KD326	$Co_{0.12}Ir_{0.88}Sb_3$ + 0.2 at.%Pt	11.6	2,53 x10^{20}	0.2	-110
1DD345	$Co_{0.94}Ir_{0.06}Sb_3$ + 0.2 at. %Te	3.8	2.68 2.68Xx 10^{19}	70	-310
2DD344	$Co_{0.94}Ir_{0.06}Sb_3$ + 0.2 at.%Pt	2.8	4.17x 10^{19}	53.8	-266
4DD347 "	$Co._{88}Ir_{0.12}Sb_3$ + 0.2 at.%Pt	2.95	3.08 x10^{19}	57.9	-295
1DD338	$Co._{88}Ir_{0.12}Sb_3$ + 0.2 at.%Te	3.5	2.96X 10^{19}	"58.9	-270

The Hall mobility for the Ir-rich solid solution samples arc low likely because conduction by both electron and hole occur in these samples, resulting in relatively large electrical resistivity values and low Seebeck coefficient values (scc Table 1). The high carrier concentrations measured on these samples are not extrinsic carrier concentrations.

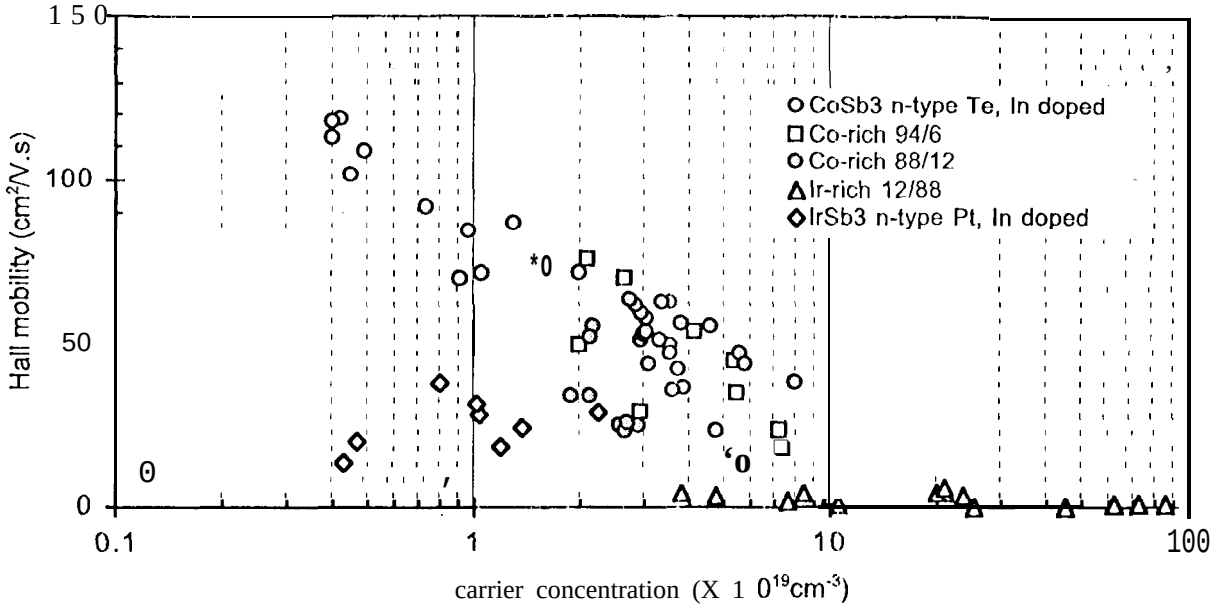

FIGURE 1. Room temperature I Ian mobility values as function of carrier concentration for n-type $IrSb_3$, $CoSb_3$, CoO.12]r08Nb3, $Co_{0.94}Ir_{0.06}Sb_3$ and CoO.88]r012Sb3 solid solutions.

It is clear however that Co-rich solid solution samples have much better Hall mobilities than samples of the Ir-rich solid solution. 1 Ian mobilities values for Co-rich solid solution samples arc actually c1osc to those measured for n-typc $CoSb_3$ at the same doping level. The decrease in carrier mobility expected in solid solutions is lcss pronounced for these n-type solid solutions than for their p-type analogs (Borshchevsky et al., 1995) because of the large difference between hole and electron mobility in these materials. As a result of the higher electron mobilities for Co-rich solid solution samples, their electrical resistivity values arc much lower than for Ir- rich solid solution samples.

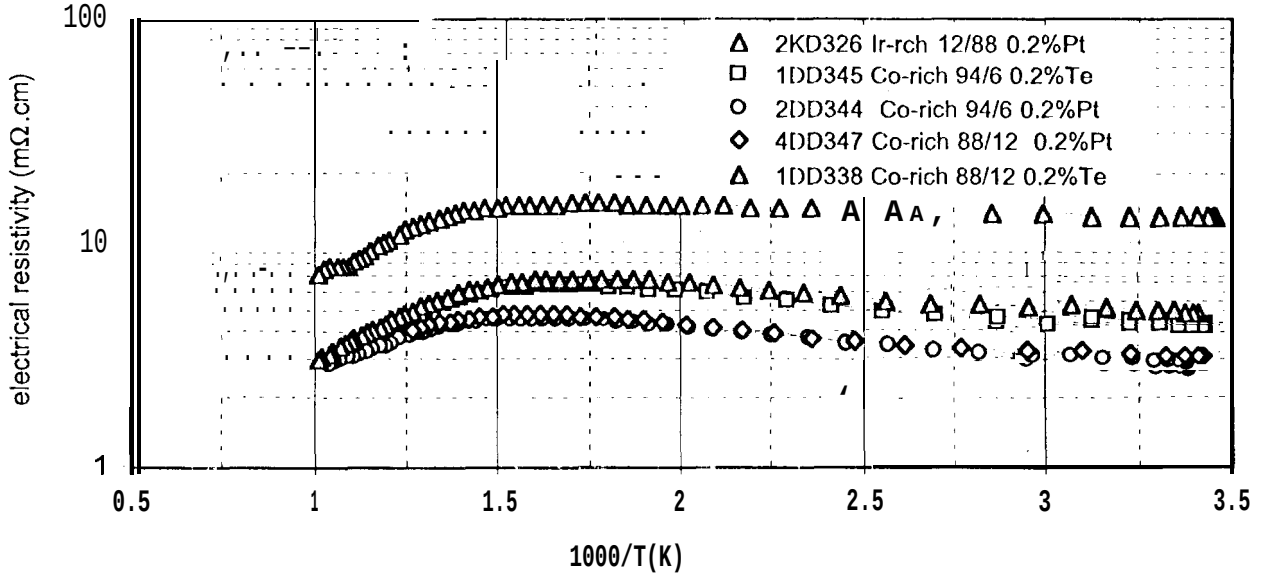

FIGURE 2. Electrical resistivity values as function of inverse temperature for n-type $Co_{0.12}Ir_{0.88}Sb_3$, $CoO_{.94}Ir_{0.06}Sb_3$ and $Co_{0.88}Ir_{0.12}Sb_3$ solid solutions

The room temperature Seebeck coefficient values for Co-rich solid solutions range from - 200 to 350 μV/K, in agreement with the results obtained on n-type $IrSb_3$ and $CoSb_3$. This indicates that, as expected, the electron effective masses are much larger than the hole masses in $Co_xIr_{1-x}Sb_3$ solid solutions. Good power factor ($\alpha^2\sigma$) values are obtained for the Co-rich solid solution samples and a maximum room temperature value of about 25 $\mu W.cm^{-1}.K^{-2}$ was calculated for a sample at a doping level of about 3 x 10'9 cm^{-3}. Figure 2 shows the high temperature values of the electrical resistivity as a function of inverse temperature for several samples of Co- and Ir-rich solid solutions. The resistivity increases with temperature up to about 400°C and then decreases due to increasing minority carrier (holes) conduction. The corresponding Seebeck coefficient values are shown in Figure 3.

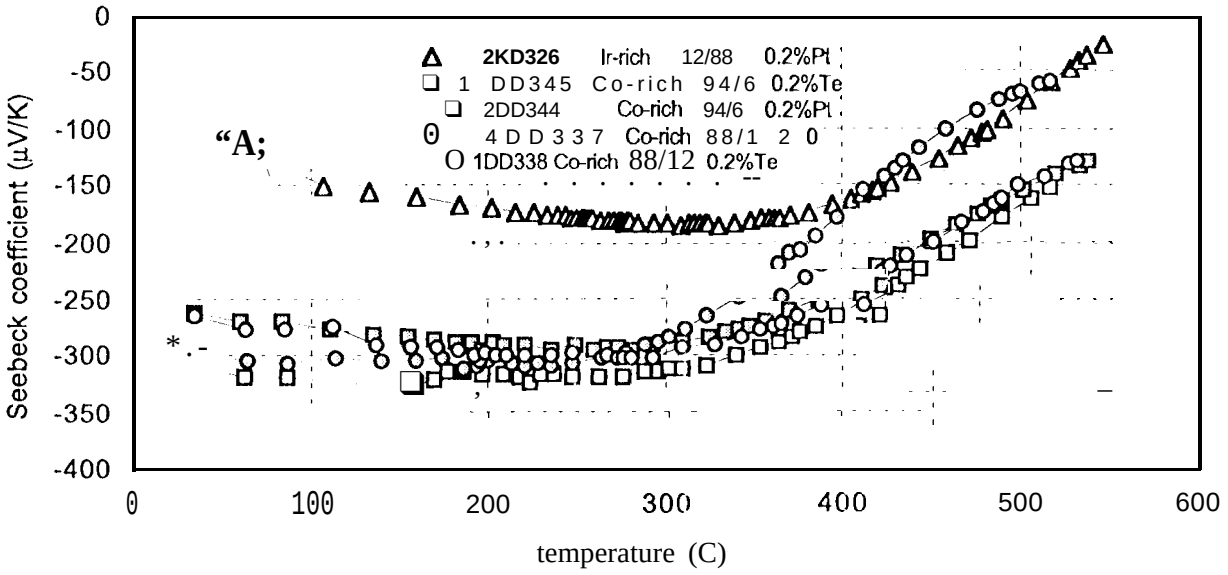

FIGURE 3. Seebeck coefficient values as function of temperature for n-type $Co_{0.12}Ir_{0.88}Sb_3$, $Co_{0.94}Ir_{0.06}Sb_3$ and $Co_{0.88}Ir_{0.12}Sb_3$ solid solutions.

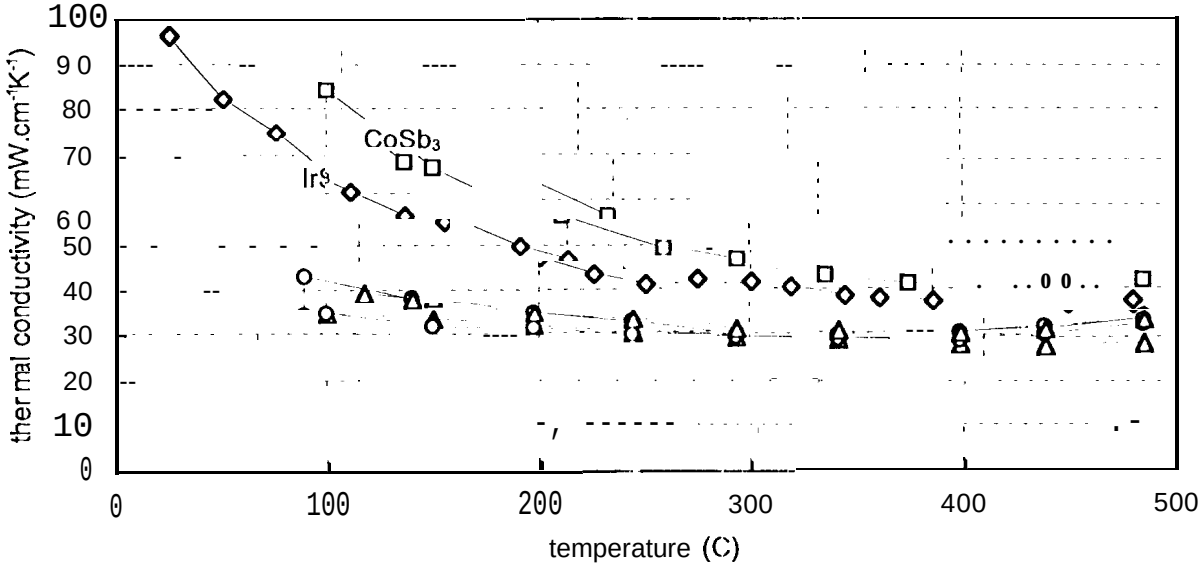

FIGURE 4. Thermal conductivity values as function of inverse temperature for n-type $IrSb_3$, $CoSb_3$, $Co_{0.12}Ir_{0.88}Sb_3$ (A) and $Co_{0.88}Ir_{0.12}Sb_3$ (O) solid solutions.

The values are large for Co-rich solid solutions and are similar to the variations observed for n-type $CoSb_3$ (Caillat et al., 1995b). The Seebeck coefficient is nearly constant up to 300°C for Co-rich solid solution samples and

decreases for higher temperatures due to conduction by minority carriers. The decrease in thermal conductivity is illustrated in Figure 4 where typical thermal conductivity values for the binary compounds $IrSb_3$ and $CoSb_3$ are compared with the thermal conductivity values for several Co-rich solid solution samples. The increased point defect scattering results in substantial decrease in thermal conductivity. The thermal conductivity of the alloys is nearly temperature independent and has a value of about 30 $mW.cm^{-1}.K^{-1}$ between 200 and 500°C. These values are in agreement with the results obtained on p-type solid solutions (Borshchevsky et al., 1995). The values are not very different for the two compositions investigated. The thermoelectric figure of merit (ZT) was calculated for several samples and a maximum value of about 0.4 was obtained at a temperature of about 300°C. This is a significant improvement compared to the results obtained on n-type $IrSb_3$ and $CoSb_3$ samples. This is due to a combination of a significant reduction in thermal conductivity with a relatively small reduction in carrier mobility. Further improvements might be expected with optimization of the doping level. Indeed, the lowest electrical resistivity measured on n-type samples was about 2.8 mΩ cm. Future work should focus on preparing n-type Co-rich solid solution samples with higher doping levels in order to obtain electrical resistivity values of the order of 1 mΩ.cm. Preliminary results suggest that ZT values of about 1 or larger could be obtained in the 200 to 500°C temperature range for samples with an electrical resistivity of about 1 mΩ.cm.

CONC1,US1ON

We prepared and measured some properties of n-type solid $In_xCo_{1-x}Sb_3$ solutions. The increased point defect scattering resulted in a substantial reduction in thermal conductivity for the solid solutions. In addition, n-type skutterudite materials seem to have a better potential for thermoelectric applications because the electron effective masses are much larger than the hole effective masses in the materials, resulting in larger Seebeck coefficient values. A maximum value of about 0.4 was measured at a temperature of about 300°C. Further improvements of the figure of merits of these solid solutions are possible with optimization of preparation technique and doping level, and this promising system should be investigated further.

Acknowledgments

This work was carried out at the Jet Propulsion Laboratory/California Institute of Technology, under contract with the National Aeronautics and Space Administration. The authors wish to express their gratitude to Jim Kulleck for X-ray analyses and Paul Carpenter for microprobe analysis.

References

Borshchevsky A., J. -P. Fleurial, E. Allevato., and T. Caillat (1995), "$CoSb_3$-$IrSb_3$ Solid Solutions: Preparation and Characterization," *Proceedings of XIIIth International Conference on Thermoelectrics*, Kansas City, MO, USA, AIP Conference 316, edited by B. Mathiprakasam: 31-34.

Caillat, T., A. Borshchevsky, and J. -P. Fleurial (1992), "Thermoelectric Properties of a New Semiconductor: $IrSb_3$," *Proceedings of XIth International Conference on Thermoelectrics*, University of Texas at Arlington, October 7-9:98-101.

Caillat, "T., A. Borshchevsky, and J. -P. Fleurial (1995a), "Preparation and Thermoelectric Properties of p- and n-type $IrSb_3$," *Proceedings of XIIIth International Conference on Thermoelectrics*, Kansas City, MO, USA, AIP Conference 316, edited by B. Mathiprakasam: 31-34.

Caillat, T., A. Borshchevsky, and J. -P. Fleurial (1995b), "Preparation And Thermoelectric Properties of p- and n-type $CoSb_3$," *Proceedings of XIIIth International Conference on Thermoelectrics*, Kansas City, MO, USA, AIP Conference 316, edited by B. Mathiprakasam: 58-61.

Morelli, D. T., T. Caillat, J. -P. Fleurial, A. Borshchevsky, J. W. Vandersande, B. Chen, and C. Uher (1995), "Low -Temperature Transport Properties of p-type $CoSb_3$," *Phys. Rev. B*, 50:9622-9628.

Morelli, D. T., and G. P. Meisner (1995), "Low Temperature Properties of the Filled Skutterudite $CeFe_4Sb_{12}$," *J. Appl. Phys.*, 77:3777-3781.

Nolas, G. S., G. A. Slack, T. M. Tritt, and D. T. Morelli (1995), "New Materials for Thermoelectric Cooling Based on $IrSb_3$," *Proceedings of XIVth International Conference on Thermoelectrics*, St. Petersburg, Russia, to

bc published.

Tritt, T. M., 1). J. Gillespie, A. C. Ehrlich, G. S. Nolas, G. A. Slack, and J. L. Cohn (1995), "Low Temperature Transport Properties of $IrSb_3$," *Proceedings of XIVth International Conference on Thermoelectrics*, St. Petersburg, Russia, to bc published,

FILTER METHODOLOGY

The filtering was performed with the GPS Inferred Positioning System Orbit Analysis and Simulation Software (GIPSY-OASIS) set developed by the Tracking Systems and Applications Section at the Jet Propulsion Laboratory, The standard filter configuration used for MOE production is of the U-D factorized batch sequential filter, Nominally, MOES based on GPS data are created from a 30 hour data fit; SLR-only solutions are created from a three-day data fit. Solutions from adjacent days would thus have an overlap ranging from 6 to 48 hours, depending on the data type combinations used. This overlap provides an opportunity to perform a quality check upon the latter solution. Under normal conditions, the overlap agrees in the radial component to well under ten centimeters RMS.

There arc five data combination scenarios which can occur during MOE production: (i) GPS (AS on) & SLR, (ii) GPS (AS off) & SLR, (iii) GPS (AS on), (iv) GPS (AS off), and (v) SLR only. For solutions involving only SLR data, the filter strategy is essentially the same as that for the original SLR-only "quick-look" orbits, covered in Reference 2. For solutions involving GPS data, the basic GPS orbit determination strategy usually involves the simultaneous adjustment of: the GPS and T/P orbits, station and satellite clock parameters, selected station locations, zenith tropospheric delays, and solar pressure coefficients (scale factors and Y-Bias), and car-rim phase biases. If the GPS constellation were to provide non-AS data, this would be the nominal strategy. In practice however, AS data is the norm, so it is more reliable to first solve for the GPS orbits and clocks, then determine the T/P orbit using the previously determined GPS orbits. With the GPS orbits fixed, solving for the T/P orbit (and GPS clocks to account for Selective Availability) with Anti-Spoofing data becomes more reliable. This two-part process is used regardless of the AS status; with a similar effort underway for the GPSMET mission (see Reference 4), there is the possibility of consolidating efforts by only generating one set of GPS orbits for both orbit determination efforts. As an additional note, to save processing time, no reduced dynamic iterations are performed in MOE production.

The data editing process does change with the AS status; when AS is on, pseudorange observable are only used in editing and not in parameter estimation. The origin of this technique comes from work performed in the Tracking Systems and Applications Section at JPL (see Reference 3). The data editing process for AS data, as well as the two-step approach to orbit determination with AS data was refined and automated by Ronald Muellerschoen; Reference 4 gives a detailed description of this process, and how it has been successfully applied to the TOPEX/Poseidon and GPSMET missions.

Another approach to handling GPS data in Anti-Spoofing Mode, but not currently used by the PVT at present, is given in Reference 5. An approximation of the ionosphere above T/P was obtained by differencing the single frequency carrier phase and pseudorange measurements. This difference was then smoothed with cubic splines and applied to the observables as a rough ionosphere calibration.

ORBIT D ETERMINATION EVALUATION

The MOEs are evaluated by their comparison to the independently determined and highly accurate POE orbits used for GDR production. In order to demonstrate the proof-of-concept of using GPS Anti-Spoofing data to the T/P project, a battery of solutions using different data type combinations was created over a complete 10 day cycle. Two methods arc used to evaluate these solutions. First, their agreement with the GSFC POE is examined, with the radial and 3-dimensional RSS values of the comparison being the

significant quantities. This comparison is valid since the original intent of the MOE is to provide the science community a working orbit for IGDR interpretation, as a prelude to the final GDR product which is based on the POE. Since the model structure of both the MOE and POE are similar, this comparison is not heavily corrupted by modeling differences. Second, the POE itself is only an approximation to the truth. Thus, it is necessary to find a quality measure which is orbit independent. The crossover variances of these orbits is such a measure, since high variances indicate corruption of altimeter data by geographically-correlated orbit error, all else being the same.

In addition to the proof-of-concept results, MOEs recently created for IGDR production are compared to the corresponding POE. At the time this document was being prepared, crossover results for these MOEs would still not be available for another month. However, radial and 3-D differences are reported for MOEs created with GPS AS and non-AS data against the POEs.

Proof-of-concept Results

To demonstrate the validity of incorporating GPS Anti-Spoofing data into MOE production, orbits were created from 22 February 199S to 04 March 199S (T/I' cycle 90). The GPS constellation was in Anti-Spoofing mode this cycle. Also, the T/P spacecraft passed from one attitude regime to another (fixed yaw to yaw steering); providing a typical level of spacecraft activity to be encountered during most cycles.

The set of solutions collected for this demonstration include the following: (i) the GSFC JGM-3 POE based on the latest models listed in Table 1[1], (ii) the GSFC JGM-2 POE, which was actually used for the original cycle 90 GDR, (iii) the JGM-2 SLR-only MOE, which was actually used for the cycle 90 IGDR, (iv) a JGM-3 SLR-only orbit, (v) a JGM-3 GPS-only (dynamic fit) orbit, and (vi) a JGM-3 GPS/SLR (dynamic fit) orbit. Orbits (iii) -(vi) were created at JPL by the PVT.

Orbits (ii) -(vi) arc differenced against the GSFC DORIS/SLR JGM-3 POE (see Figure 2), which is considered the most accurate of the set. The comparison of the JGM-2 and JGM-3 POES demonstrates the magnitude of the orbit solution change brought about by the geodetic model updates. Likewise, going from the JGM-2 to JGM-3 SLR-only solutions shows some improvement in the agreement, but not as much as the DORIS/SLR solutions. The GPS-only solution has a level of agreement similar to the SLR-only solution; bringing the two data types together results in an orbit that approaches the JGM-2 POE agreement with the JGM-3 POE.

[1] In the update to the models used for MOE and POE production, the change of gravity field (from JGM-2 to JGM-3) yields (he most dramatic reduction in geographically correlated orbit error. As a result, orbits based on the former model set are referred to as the "JGM-2" orbits, and those using the later models arc referred to as "JGM-3" orbits.

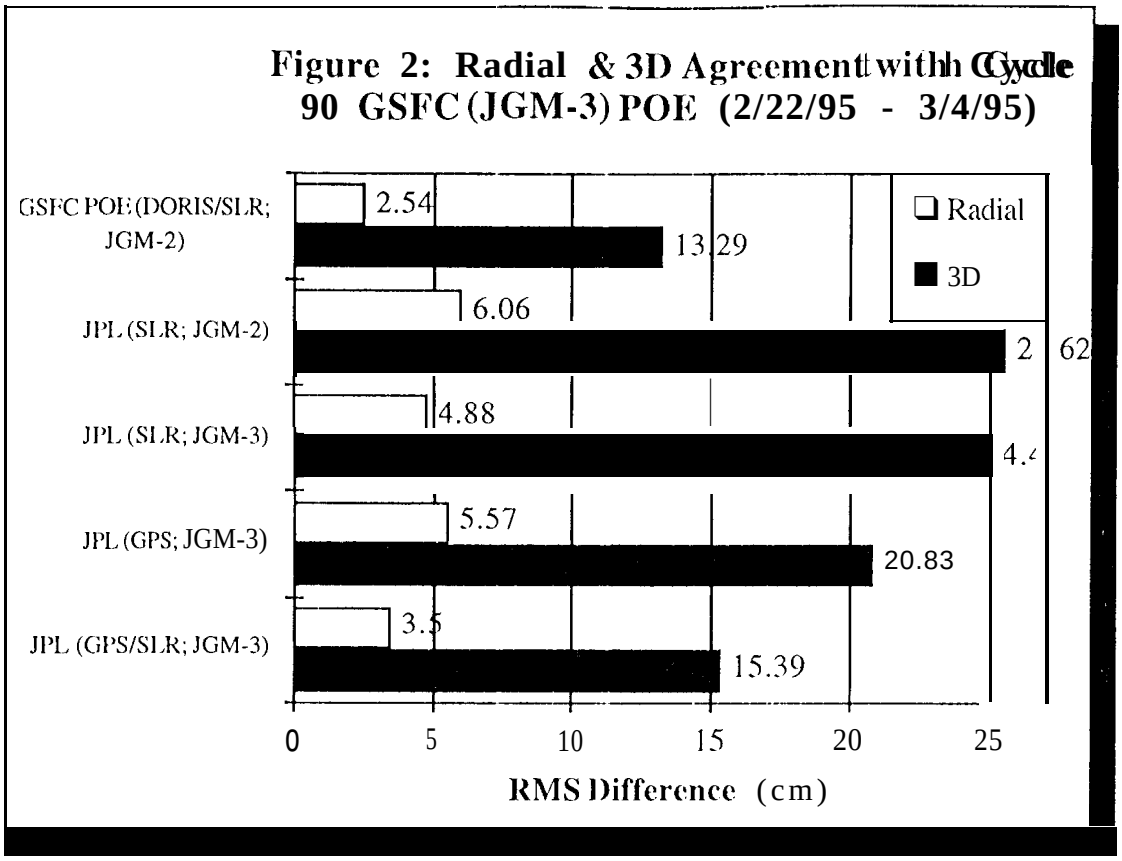

The altimeter crossover results (see Figure 3) tell a similar story. The model improvements result in lower crossover variances in both the DORIS/SLR and SLR-only fits. The combination of GPS and SLR data result in an orbit with a crossover variance approaching that of the JGM-2 POE.

Figure 3: T/P Altimeter Crossovers: Cycle 90 (22 February - 04 March 1995)

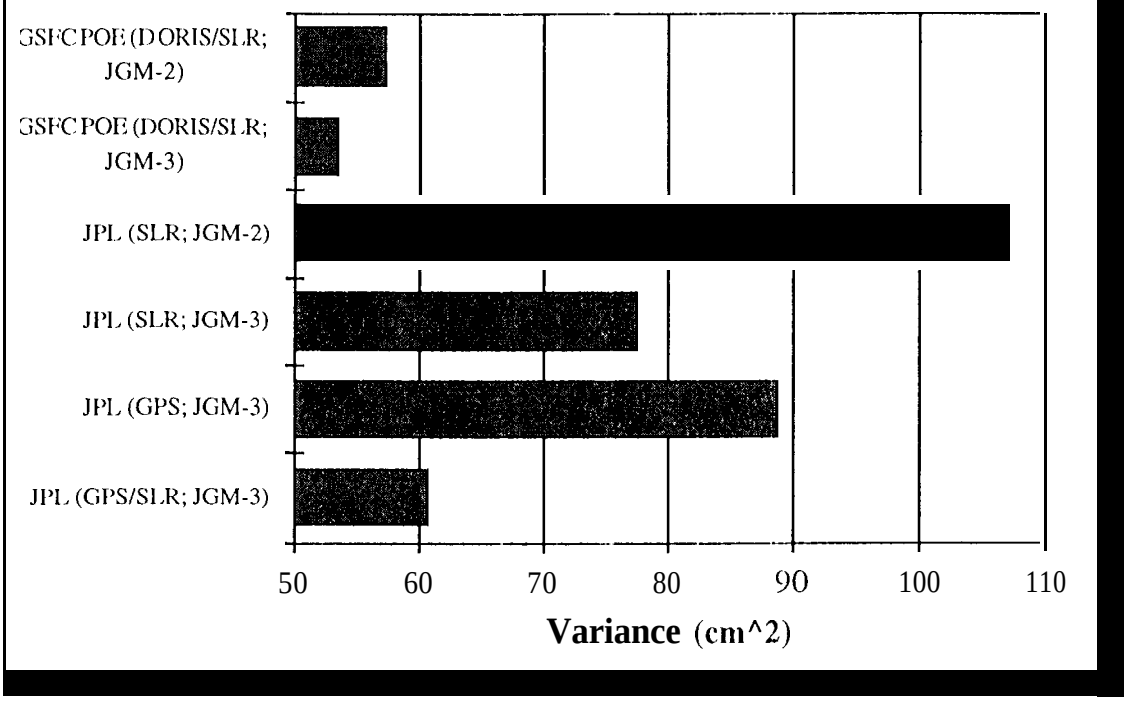

A parallel battery of solutions is not yet available for a cycle in which Anti-Spoofing was turned off. However, a GPS/SLR orbit was created for cycle 43 which has many of (he characteristics of an MOE (JGM-3 models, dynamic fit only, GIPSY-OASIS software). The crossover variance from that orbit (see Figure 4) is slightly lower than that for the JGM-3 GSFC POE. The next opportunity to compare MOE and POE crossovers for an non-AS (3PS constellation will be after the creation of the merged GDRs for 21 June -01 July 1995 (T/P cycle 102).

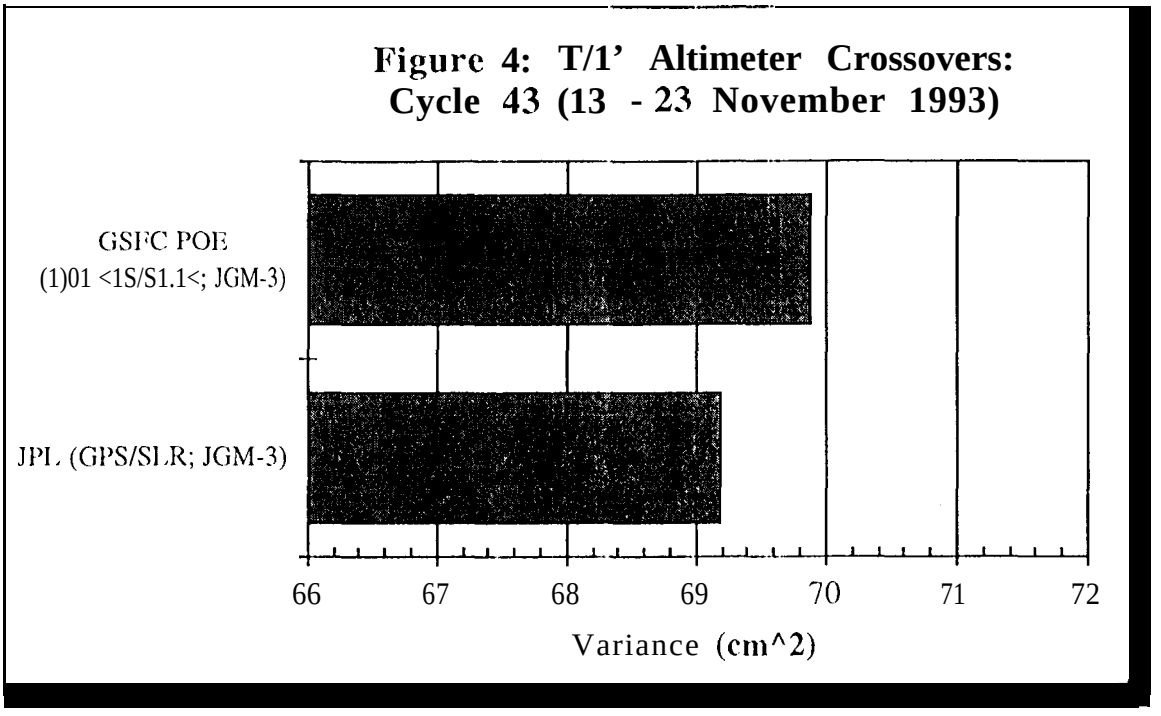

Actual **MOE** Results

The new GPS/SLR MOE production mode began with the start of Cycle 100 on 01 June 1995. From late May to late June 1995, MOE production passed through three of the five possible data type combinations: SLR-only (with JGM-2 models), GPS(AS on)/SLR, and GPS(AS off)/SLR. These orbits, which span cycles 99-102, are compared to their corresponding POE. In Figure 5, the radial RMS agreement between MOEs and POEs is plotted for the daily solution. The trend amongst the three different solution types is as expected, with the GPS (non-AS)/SLR solution having the best agreement with its corresponding POE. The difference in the agreement between the MOEs with AS GPS data and those with non-AS GPS data can be considered a measure of the orbit degradation brought about by the ionosphere. Nevertheless, the GPS (AS)/SLR solutions are still an improvement over the SLR-only JGM-2 MOEs. likewise, Figure 6 shows the same trend for three-dimensional comparisons of the orbits.

Figure 5: Radial Orbit Differences Between JPL MOEs and GSFC (JGM-3) POEs

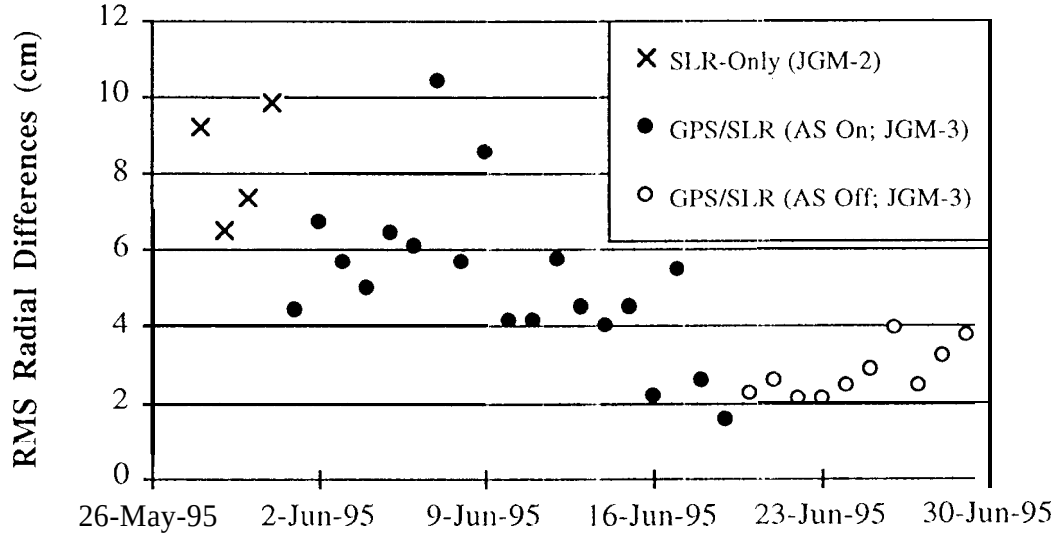

Figure 6: 3D Orbit Differences Between JPL MOEs and GSFC (JGM-3) POEs

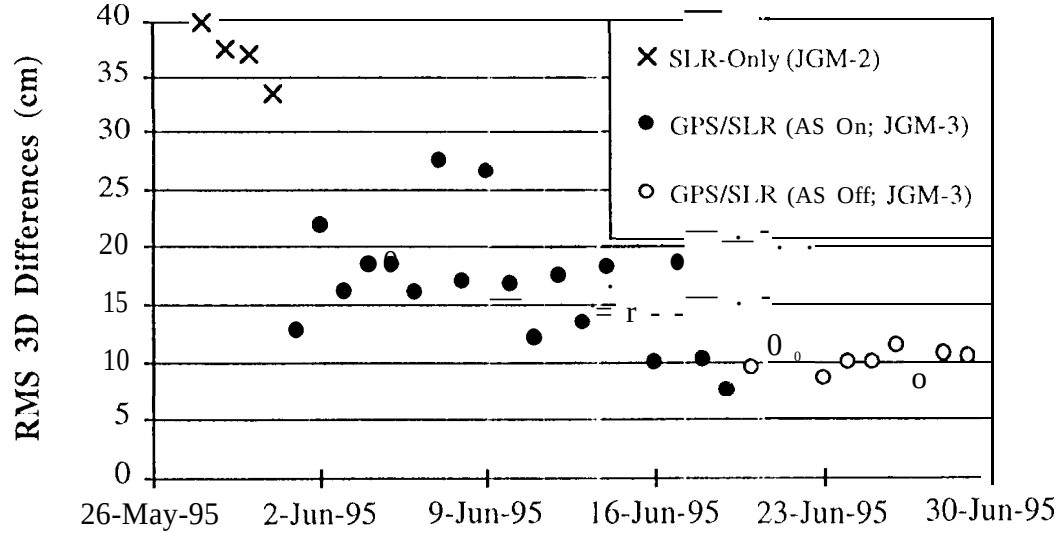

SUMMARY

The PVT has not only met the mission requirement of sub-decimeter accuracy throughout the l/P prime mission, it has both improved the quality of its orbits and removed its vulnerability to a single data type with this upgrade, all with minimal resources and no interruption to mission operations. This paper documents the cooperative effort between the Tracking Systems and Applications Section and the Navigation and Flight Mechanics Section to provide precision orbits with minimal resources. Orbit comparisons ant] crossover statistics show that the accuracy of these "quick-look" orbits approaches that of the POEs supplied to the project during most of the prime mission, even under the degrading effects of Anti-Spoofing.

ACKNOWLEDGMENTS

The research described in this paper was carried at the Jet Propulsion Laboratory, California Institute of Technology, under contract with the National Aeronautics and Space Administration.

REFERENCES

1. TOPEX/Poseidon POD Team, "Precision Orbit Reprocessing for the Improved MGDR," Memorandum, University of Texas at Austin, 28 March 1995,

2. Cangahuala, L. A., Christensen, E. J., Graat, E. J., Williams, B. G., Wolff, P. J., "TOPEX/Poseidon Precision Orbit Determination: 'Quick-Look' Operations and Orbit Verification," Paper AAS 95-228 presented at AAS/AIAA Spaceflight Mechanics Meeting, Albuquerque., NM, 13-16 February, 1995.

3. Blewitt, G. and Lindqwister, U., "GPS Parameter Estimation with Constrained Carrier Phase Biases," JPL Internal Memorandum 335.4-88-149, 1988,

4. Muellerschoen, R. J., Lichten, S., and Lindqwister, U., "Results of an Automated GPS Tracking System in Support of TOPEX/Poseidon and GPSMET, " to be presented at ION Meeting, Palm Springs, CA, September 1995.

5. Guinn J. R., Jee, J. R., Munson, T. N., "TOPEX/Poseidon Orbit Determination Using Global Positioning Satellites in Anti-Spoofing Mode," Paper AAS 94-138 presented at AAS/AIAA Spaceflight Mechanics Meeting, Cocoa Beach, FL, 14-16 February 1994.